Optical inhibition of motor nerve and muscle activity

OPTICAL INHIBITION OF MOTOR NERVE AND MUSCLE ACTIVITY *IN VIVO*

HOLLY LISKE, MS,[1] CHRIS TOWNE, PhD,[2] POLINA ANIKEEVA, PhD,[3] SHENGLI ZHAO, PhD,[4] GUOPING FENG, PhD,[5] KARL DEISSEROTH, MD, PhD,[2,6] and SCOTT DELP, PhD[1,2]

[1]Department of Mechanical Engineering, Stanford University, Stanford, California, USA
[2]Department of Bioengineering, Stanford University, Stanford, California, USA
[3]Department of Materials Sciences and Engineering, Massachusetts Institute of Technology, Cambridge, Massachusetts, USA
[4]Department of Neurobiology, Duke University Medical Center, Durham, North Carolina, USA
[5]Department of Brain and Cognitive Sciences, Massachusetts Institute of Technology, Cambridge, Massachusetts, USA
[6]Department of Psychiatry and Behavioral Sciences, Stanford University, Stanford, California, USA

Accepted 7 October 2012

ABSTRACT: *Introduction:* There is no therapeutic approach that provides precise and rapidly reversible inhibition of motor nerve and muscle activity for treatment of spastic hypertonia. *Methods:* We used optogenetics to demonstrate precise and rapidly reversible light-mediated inhibition of motor nerve and muscle activity *in vivo* in transgenic *Thy1::eNpHR2.0* mice. *Results:* We found optical inhibition of motor nerve and muscle activity to be effective at all muscle force amplitudes and determined that muscle activity can be modulated by changing light pulse duration and light power density. *Conclusions:* This demonstration of optical inhibition of motor nerves is an important advancement toward novel optogenetics-based therapies for spastic hypertonia.

Muscle Nerve **000**:000–000, 2013

The upper motor neuron syndrome includes a constellation of symptoms caused by lesions affecting upper motor neuron pathways.[1] These lesions, which occur with cerebral palsy, stroke, and other cerebrospinal injuries, frequently give rise to abnormal activity in lower motor neurons and involuntary muscle contractions through mechanisms that remain unclear.[1–4] Spastic hypertonia, a major feature of the upper motor neuron syndrome, is characterized by exaggerated muscle activity in response to muscle stretch. Individuals with spastic hypertonia may be unable to perform voluntary movements, such as walking, and experience significant disability and reduced quality of life.[3]

Current approaches to inhibit motor nerve and muscle activity for treatment of spastic hypertonia have important limitations.[2,3] Oral medications such as dantrolene and tizanidine have poor specificity and side effects, including sedation, weakness, and withdrawal.[3] Selective dorsal rhizotomy[2] reduces spasticity through irreversible damage of the nerve. Intramuscular injection of botulinum toxin diminishes spasticity by blocking release of acetylcholine at the neuromuscular junction for a period of several months, but its use is limited by drug tolerance and muscle weakness.[3] To date, no clinical treatment provides precise and rapidly reversible inhibition of motor nerve and muscle activity to treat spastic hypertonia. Thus, a novel means for precise, reversible inhibition is a long-sought goal of neuroscience, bioengineering, and clinical research.

Optogenetics employs light-sensitive proteins encoded by microbial opsin genes to facilitate optical excitation or inhibition of metazoan neurons.[5] This method capitalizes on the precision of gene targeting of opsins to specific cell types and on the speed of optical interrogation. Two opsins, channelrhodopsin-2 (ChR2) and halorhodopsin (NpHR), have been the most widely used tools for optical deconstruction of neural circuits. When illuminated with blue light, ChR2 allows sodium ion influx into neurons causing membrane depolarization and excitation of action potentials.[6] In contrast, NpHR, when illuminated with yellow light, pumps chloride ions into neurons, hyperpolarizing the membrane and inhibiting action potentials.[7] Optical excitation and inhibition have been demonstrated in mammalian brain slices and in brains of living mice.[5] In the peripheral nervous system, ChR2-mediated optical excitation of motor nerve axons in the mouse sciatic nerve was used to achieve orderly recruitment of motor units of lower limb muscles.[8] In addition, cardiomyocytes in the mouse[9] and rat[10] and skeletal myocytes in the developing chick embryo[11] have been excited with ChR2 and blue light. There have been no reports of optical inhibition of motor nerve and muscle activity in the peripheral nervous system.

The goal of this work was to determine whether NpHR could be used in the peripheral nervous system to inhibit motor nerve and muscle activity

Abbreviations: AAV, adeno-associated virus; ChR2, channelrhodopsin-2; EMG, electromyography; eNpHR2.0, enhanced halorhodopsin version 2.0; EYFP, enhanced yellow fluorescent protein; NpHR, halorhodopsin

This article includes Supplementary Material available via the internet at http://www.mrw.interscience.wiley.com/suppmat/0148-639X/suppmat/

Supported by a Stanford Bio-X Interdisciplinary Initiatives Award, a Stanford National Institutes of Health Graduate Training Program in Biotechnology grant, a grant from the W.M. Keck Foundation, and NIH grant R01NS080954.

Key words: electromyography; halorhodopsin; optogenetics; sciatic nerve; spastic hypertonia

Additional Supporting Information may be found in the online version of this article.

Correspondence to: S. Delp; e-mail: delp@stanford.edu

Published online 00 Month 2012 in Wiley Online Library (wileyonlinelibrary.com). DOI 10.1002/mus.23696

with light. We first sought to determine whether enhanced NpHR (eNpHR2.0) is expressed in axons of the sciatic nerve of *Thy1::eNpHR2.0* mice. We next sought to demonstrate optical inhibition of muscle force and electromyographic activity and measure the time precision of inhibition. We examined inhibition over the range of electrically stimulated muscle force and characterized the dependence of inhibition on light power density.

METHODS

Histology and Expression Analysis. All animal procedures were approved by the institutional animal care and use committee at Stanford University, in accordance with the "Guide for the Care and Use of Laboratory Animals" from the National Institutes of Health. Healthy adult male and female *Thy1::eNpHR2.0* and wild-type C57BL/6 mice, ages 8–14 weeks (average mass 26 g), were studied. *Thy1::eNpHR2.0* (line 2) mice were obtained from Jackson Laboratories (Bar Harbor, Maine). eNpHR2.0 is a modified version of NpHR that has improved membrane localization and expression along neuronal processes.[12,13] The latter feature is especially relevant for controlling motor nerves, which have axons that span great distances from cell somata in the spinal cord to muscles in the periphery.

We performed histology and expression analysis of the sciatic nerve to determine whether transgenic *Thy1::eNpHR2.0* mice express eNpHR2.0 fused to enhanced yellow fluorescent protein (EYFP) in the peripheral nervous system. We perfused animals with 4% paraformaldehyde and prepared transverse 20-μm-thick nerve cryosections. For expression analysis, nerves from transgenic and control mice were processed on the same slide. Histology was performed against laminin, a basement membrane marker, as this protein is highly expressed in the peripheral nervous system and serves as a counterstain for axons. We labeled sections with a primary antibody against laminin (1:200; AL-4; Abcam, Cambridge, Massachusetts) and a secondary antibody, Cy3-conjugated donkey anti-rat (1:1000; Jackson Laboratories), using standard histological protocols. Scans in the EYFP channel were taken at 40× magnification and 2× zoom at a low gain (600 PMT) and high offset (1%) such that no fibers were saturated. Representative raw images are shown in Figure S1 (refer to Supplementary Material available online). eNpHR2.0 expression was sufficiently high so that all axons in nerves from transgenic mice were brighter than the background levels observed in axons from wild-type mice. ImageJ software was used to quantify mean fluorescence intensity and diameter of individual fibers.[14]

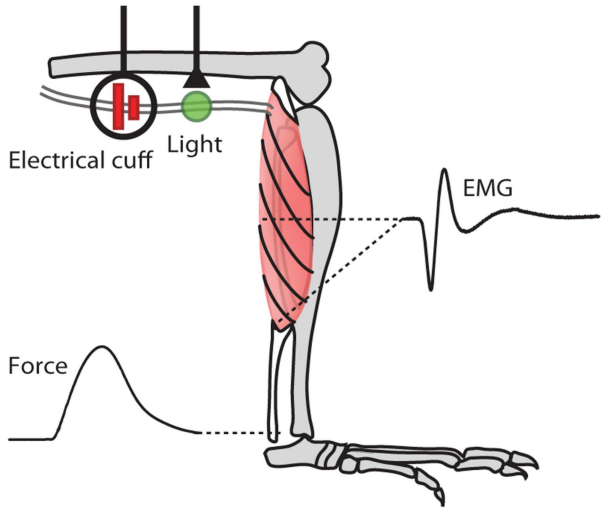

FIGURE 1. Schematic of experimental measurements. Motor axons of the sciatic nerve were stimulated electrically with a stimulation cuff placed around the proximal sciatic nerve of an anesthetized *Thy1::eNpHR2.0* mouse. The distal sciatic nerve was illuminated with green laser light (561 nm). Fine-wire EMG electrodes recorded electrical activity of the medial gastrocnemius. A force transducer attached at the Achilles tendon recorded the contractile force of the lower limb muscles. [Color figure can be viewed in the online issue, which is available at wileyonlinelibrary.com.]

***In Vivo* Measurements.** We performed a series of experiments to determine whether electrically stimulated motor nerve and muscle activity could be inhibited by illumination of the sciatic nerve in anesthetized *Thy1::eNpHR2.0* and wild-type mice. Mice were anesthetized with isoflurane (1–3%) and kept warm on an electrical heating pad (37°C). The hindlimb was shaved, and the sciatic nerve was exposed. The triceps surae muscle group of the lower limb was exposed, and the Achilles tendon was isolated. The calcaneus was cut, and a small bone piece at the tendon was attached through a lightweight, rigid hook to a force transducer (0.3-mN resolution; 300C-LR; Aurora Scientific, Aurora, Ontario). Electromyography (EMG) electrodes made from stainless steel, tetrafluoroethylene-coated wires (50 μm; 790700; A-M Systems, Carlsborg, Washington) were inserted into the medial gastrocnemius muscle belly and muscle–tendon junction with a ground electrode at the forelimb wrist.

To initiate motor nerve activity we placed a custom-built stimulation cuff around the sciatic nerve and applied electrical stimulation (Figs. 1 and S2). The sciatic nerve includes motor and sensory axons; however, only motor activity was investigated here. Electrically stimulated motor axons propagate action potentials to the lower limb muscles to cause contractile and electrical muscle activity. Contractile activity was recorded by the force transducer, and electrical activity was recorded by the EMG electrodes. To achieve

optical inhibition, we illuminated axons in the nerve 1–3 mm distal to the electrical stimulation cuff with green laser light.

Electrical Stimulation. Motor nerves were electrically stimulated (S48 Stimulator; Grass Technologies, West Warwick, Rhode Island) through the stimulation cuff. Supramaximal stimulation was determined for each mouse by incrementally increasing voltage until twitch force amplitude plateaued. Stimulation voltage was alternately increased and decreased for subsequent trials to avoid possible temporal effects. Twitch stimulation was 0.1-ms pulses at 1 Hz for 20 s. Tetanic stimulation was 0.1-ms pulses at 100 Hz for 3 s at approximately 50% of supramaximal twitch force. Rest periods were 20 s and 5 min between trials of twitch and tetanus, respectively.

Illumination. Illumination was from a diode-pumped solid-state yellow-green laser (561 nm; CrystaLaser, Reno, Nevada) via a multimode optical fiber (400-μm diameter, 0.37 numerical aperture; Thorlabs, Newton, New Jersey). The 561-nm wavelength is within 70% of the eNpHR2.0 activation peak of 589 nm.[15] Light power density was calculated as the power at the fiber tip measured with a power meter (PM100; Thorlabs) divided by the light spot area of 1.0 mm^2 illuminating the nerve (diameter of approximately 1.1 mm). The internodal length of C57BL/6 mouse sciatic nerve is approximately 0.63 mm.[16] Therefore, we expect that this light spot illuminated, on average, 1 or 2 nodes of Ranvier per axon. The angle of light incidence at the nerve surface was insufficient to cause total internal reflection, assuming the nerve refractive index is similar to that of brain.[17] We therefore expected that light would propagate transversely through the nerve with minimal longitudinal spreading. Average temperature increase at the nerve (1.4°C) during a 4-s pulse with 6.0 mW/mm^2 measured with a thermocouple (Omega, Stamford, Connecticut) was below the average temperature increase (2.1°C) related to hyperthermia-induced changes in rat hippocampal neurons after 10 min of heating (Table S1).[18] Experiments with *Thy1::eNpHR2.0* and wild-type mice involved 3–6 h of repeated electrical stimulation and illumination (up to 200 trials per mouse). We observed no localized nerve damage and no systematic change in force or EMG during this time.

Data Recording and Analysis. Force and EMG data were recorded at 10 kHz (PCI-6251; National Instruments, Austin, Texas) and analyzed using MATLAB (The Mathworks, Natick, Massachusetts). Passive force (muscle force with no activation) was measured for each trial prior to electrical stimulation of the nerve. Analyses were done on the active (total − passive) force. Average peak twitch force with light off (F_{av_off}) and light on (F_{av_on}) were calculated for each trial of 20 twitches. Percent inhibition was $(F_{av\_off} - F_{av\_on}) / (F_{av\_off}) * 100$. Average tetanic force was calculated with light off (1.1–1.9 s of trial duration, F_{av_off}) and light on (2.1–2.9 s of trial duration, F_{av_on}). Data that were collected in the 100-ms durations after light onset and light offset were excluded from calculations due to the rapid changes in force amplitude. EMG was bandpass filtered (50–300 Hz) and full-wave rectified, and percent inhibition was calculated using the same method as was used for force. EMG amplitudes were normalized to the twitch and tetanus maximum EMG amplitudes observed in that mouse.

We quantified the time precision of inhibition by measuring the time durations between light onset and inhibition of tetanic force and between light offset and reversal of inhibition. Inhibition was defined to begin when force amplitude decreased $\geq$2 standard deviations below the mean force prior to illumination, and reversal was defined to occur when force amplitude increased $\geq$2 standard deviations above the mean force during illumination.

Statistics. Standard error of the mean (SEM) was calculated from the variance of the mean calculated for each mouse. *P*-values were calculated for unequal sample size and unequal variance using a Welch *t*-test (two-sided, $\alpha < 0.01$) with degrees of freedom calculated using the Welch–Satterthwaite equation.

RESULTS

Optical Inhibition of Motor Nerve and Muscle Activity in *Thy1::eNpHR2.0* Mice. *Thy1::eNpHR2.0* mice express eNpHR2.0-EYFP at high functional levels throughout the brain,[12] and we found that these mice also express eNpHR2.0-EYFP in the peripheral nervous system. Confocal microscopy of EYFP fluorescence revealed high levels of eNpHR2.0 expression within nearly all axons (>99%) of the sciatic nerve (Fig. 2A). eNpHR2.0-EYFP appeared localized to neuronal membranes (Fig. 2B). However, we observed variability in the level of expression across the neuronal population (Fig. 2B and Fig. S1). No correlation was found between axon diameter and level of expression ($r^2 = 0.11$).

We observed robust and reversible inhibition of electrically stimulated twitch and tetanic muscle force and EMG by illuminating the sciatic nerve with pulses of green light (Fig. 3A and B). Twitch force and EMG amplitudes were inhibited during 4-s light pulses and returned to prior magnitudes upon cessation of each light pulse. Representative traces show >90% inhibition of twitch force and EMG. Representative traces show 48% inhibition

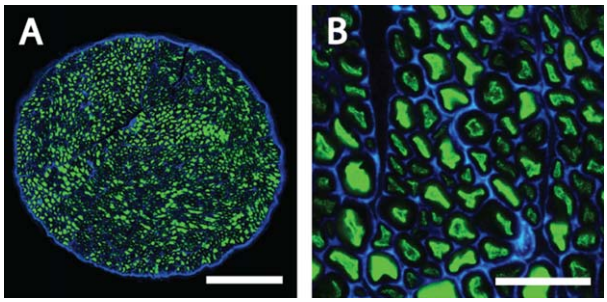

FIGURE 2. eNpHR2.0 expression in the sciatic nerve. **(A)** Confocal image of a *Thy1::eNpHR2.0* mouse sciatic nerve in cross-section showing motor nerve axons expressing eNpHR2.0-EYFP (green). An antibody against laminin (blue) labels glial cells surrounding neurons. Scale bar: 100 μm. **(B)** eNpHR2.0-EYFP appears localized to the membranes of motor nerve axons; staining as in **(A)**. Scale bar: 20 μm.

of tetanic force and 77% inhibition of EMG during a 1-s light pulse. Thus, optical inhibition of motor nerve activity is possible and causes substantial and reversible inhibition of electrically stimulated muscle activity.

We measured the times between onset and offset of the light pulse and inhibition of tetanic force to quantify the time precision of optical inhibition. Inhibition of tetanic force occurred 65 ± 18 ms after light onset, and reversal of inhibition occurred 38 + 5 ms (mean ± SEM) after light offset (n = 4 mice, 30 trials).

Inhibition over the Range of Electrically Stimulated Force. We quantified inhibition of twitch force and EMG amplitudes in *Thy1::eNpHR2.0* mice and wild-type mice (Fig. 4A and B) at force amplitudes

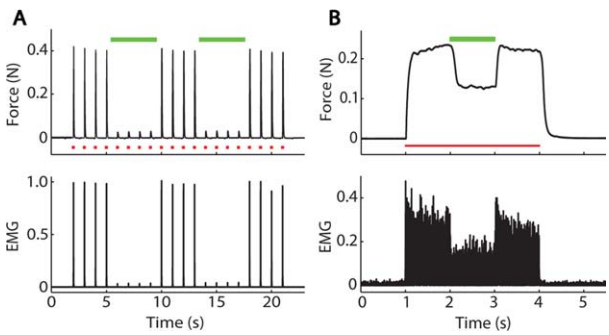

FIGURE 3. Demonstration of optical inhibition. **(A)** Example force and EMG data recorded during muscle twitches elicited by 20 s of 1-Hz supramaximal electrical stimulation (0.1-ms pulse duration, red squares, n = 1). EMG was full-wave rectified, filtered, and normalized to the twitch and tetanus maximum amplitudes recorded during the experiment. Average force and EMG amplitudes were inhibited reversibly by 93% and 96%, respectively, during 2 pulses of green light (4-s pulse duration, 14.6 mW/mm^2, green bars). **(B)** Example force and EMG data during muscle tetanus elicited by 3 s of 100-Hz 50% supramaximal electrical stimulation (0.1-ms pulse duration, red line, n = 1). Average force and EMG amplitudes were inhibited by 48% and 77%, respectively, during a pulse of green light (1-s pulse duration, 14.6 mW/mm^2, green bar).

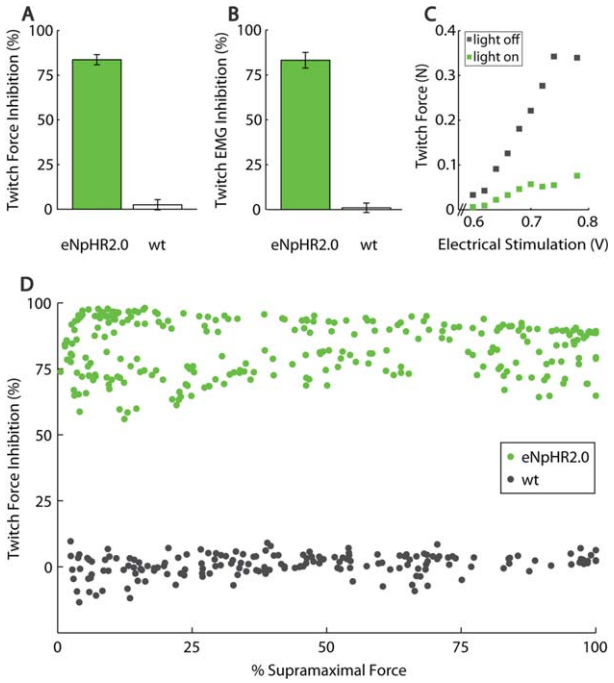

FIGURE 4. Inhibition of minimum to maximum electrically stimulated muscle activity with green light (6.0 mW/mm^2). **(A)** Percentage force inhibited by light in *Thy1::eNpHR2.0* mice (n = 5 mice, 21 trials) and wild-type mice (wt; n = 3 mice, 20 trials). Peak twitch force without illumination was 50% of supramaximal in all trials. Error bars show mean ± SEM. **(B)** Percentage EMG magnitude inhibited as in **(A)**. **(C)** Representative motor unit recruitment curves of a *Thy1::eNpHR2.0* mouse without and with illumination of the nerve. Each point represents average peak twitch force during 1 trial (n = 1 mouse). **(D)** Percentage force inhibited as in **(A)** over the range from minimum to maximum electrically stimulated force in *Thy1::eNpHR2.0* mice (n = 5 mice, 273 trials) and wild-type mice (n = 3 mice, 176 trials). Each point represents average percent inhibition of 1 trial.

of approximately 50% of supramaximal force. Illumination of the sciatic nerve with a light power density of 6.0 mW/mm^2 was sufficient to cause inhibition in *Thy1::eNpHR2.0* mice (mean ± SEM: 83 ± 3% and 84 ± 4% for force and EMG, respectively), indicating a significant difference from wild-type mice (P = 0.0000059 and 0.000087 for force and EMG, respectively).

Without illumination, increasing stimulation voltage increased twitch force amplitudes to generate a characteristic electrically stimulated motor unit recruitment curve. During illumination, we observed 81% inhibition of the plateau region of the recruitment curve. The representative curves demonstrate inhibition exceeding 74% at all amplitudes of twitch force (Fig. 4C).

To further establish the relationship of inhibition to force amplitude we determined percent inhibition over the range of electrically stimulated twitch forces in *Thy1::eNpHR2.0* and wild-type mice (Fig. 4D). We found effective inhibition at all

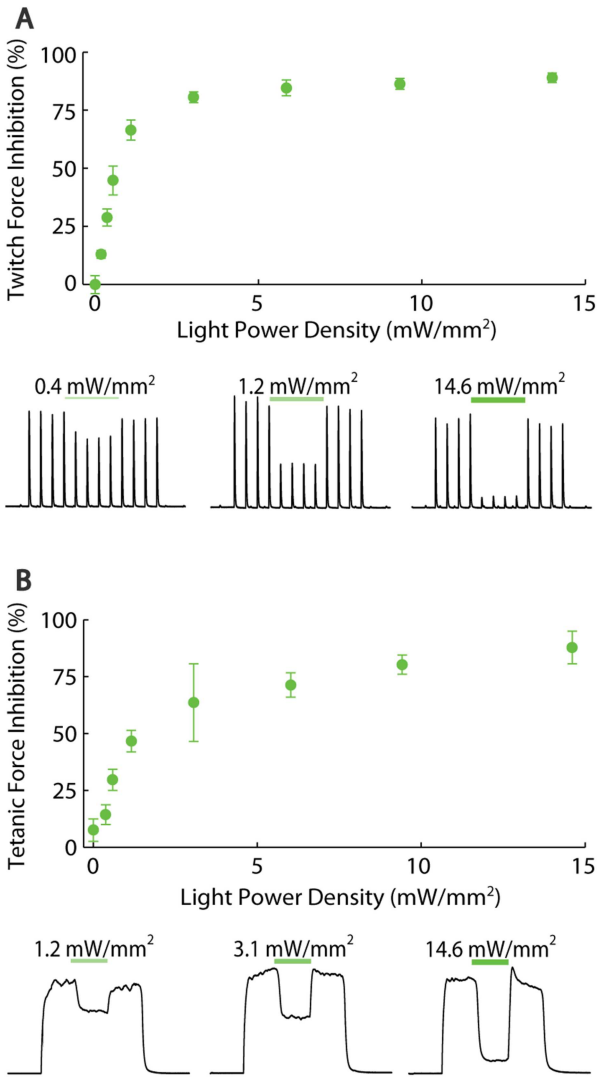

FIGURE 5. Modulation of inhibition with light power density. Peak force without illumination was 50% of supramaximal twitch force in all trials. **(A)** Percent inhibition of twitch force in *Thy1::eNpHR2.0* mice (n = 5 mice, 239 trials). Each point represents mean ± SEM. Example force twitches show 26%, 61%, and 88% inhibition with 0.4, 1.2, and 14.6 mW/mm^2, respectively. **(B)** Percent inhibition of tetanic force in *Thy1::eNpHR2.0* mice (n = 4 mice, 64 trials). Each point represents mean ± SEM of 8 trials. Force decline due to fatigue was responsible for nonzero (8%) inhibition at 0 mW/mm^2. Example force trains show 29%, 42%, and 85% inhibition at 1.2, 3.1, and 14.6 mW/mm^2, respectively. [Color figure can be viewed in the online issue, which is available at wileyonlinelibrary.com.]

amplitudes of twitch force with an average percent inhibition of 80 ± 6%. Illumination did not cause inhibition in wild-type mice (average percent inhibition = 1 ± 4%). This relationship suggests that optical inhibition may effectively reduce both chronic, low-level muscle activity and brief bursts of high muscle activity.

Relationship between Optical Inhibition and Light Power Density. We found that the degree of inhibition of twitch force was directly related to light power density. As illumination was increased incrementally up to 1.2 mW/mm^2, twitch force inhibition increased to 66 ± 2% (Fig. 5A). The average slope in this region was 57% per mW/mm^2. As illumination was further increased to 14.6 mW/mm^2, inhibition increased more modestly to 89 ± 1%, with an average slope of 1% per mW/mm^2. In the Supplementary Material, we provide a video demonstration of increasing inhibition of twitch force with increasing light power density (Video S1 and Fig. S3).

Tetanic forces were also modulated with illumination. As illumination was increased incrementally up to 1.2 mW/mm^2, inhibition increased to 47 ± 5% (Fig. 5B). The average slope in this region was 34% per mW/mm^2. As illumination was further increased to 14.6 mW/mm^2, inhibition increased to 88 ± 7%, with an average slope of 2% per mW/mm^2.

DISCUSSION

In this study we have demonstrated NpHR-mediated optical inhibition of motor nerve and muscle activity in the peripheral nervous system. We found that illumination of the sciatic nerve with 561 nm laser light causes robust and reversible inhibition of motor nerve activity and significantly reduces muscle force and EMG in *Thy1::eNpHR2.0* mice. The data show that eNpHR2.0 is capable of intercepting spikes in the axon, optical inhibition is effective at all amplitudes of electrically stimulated twitch force, and light power density modulates the degree of inhibition. The results demonstrate the potential of NpHR as a powerful tool for inhibiting motor nerve and muscle activity with light. Combined with optical excitation of muscle via illumination of ChR2-expressing motor nerve axons,[8] our method for optical inhibition of muscle activity creates a powerful toolbox for temporally precise control of peripheral nerves and muscles with light.

Greater than 1 mW/mm^2 is required to activate eNpHR2.0, and light power density is reduced due to scattering and absorption when light is transmitted through rat and mouse cortex.[13,19] Our results in mouse sciatic nerve suggest that increasing light power density at the nerve surface activates eNpHR2.0 through greater depths of the nerve cross-section. Percent inhibition increased most dramatically as light power density became sufficient to activate eNpHR2.0 throughout the nerve cross-section. Thus, we identified changing the light power density as a means to modulate the degree of inhibition of motor nerve and muscle activity. Further advancement of optical inhibition in the peripheral nervous system will require characterization of this relationship for nerves with different diameters and comparing various means to deliver light to the nerve.

Optogenetic approaches have facilitated the deconstruction of numerous neural circuits in the brain[5] and may allow us to gain understanding of

neural circuits in the peripheral nervous system and the diseases associated with them. Peripheral nerves can be excited with electrical stimulation and inhibited with high-frequency alternating current,[20,21] but these electrical methods have limited ability to control activity in selected nerve pools. Although these results were obtained in transgenic mice in which nearly all nerves were sensitive to light, optogenetic methods enable activation and inhibition of selected nerves by utilizing viral targeting of opsins to these nerves.[5] For example, optogenetics enabled systematic targeting of different elements of the Parkinson disease circuit.[22] Selective optical stimulation in layer V of motor cortex was found to ameliorate parkinsonian symptoms, elucidating underlying mechanisms of therapy with deep brain stimulation. Future work that enables cellular-level optogenetic control of specific motor nerves may allow dissection of the neural circuits involved in spasticity and provide a novel means to elucidate the mechanisms of spasticity.

Development of optogenetics-based therapies will require selective, virus-mediated gene delivery of NpHR or other opsins to non-transgenic motor nerves in humans. Selective virus-mediated gene delivery of fluorescent protein to distinct motor neuron pools has been achieved in rodents and nonhuman primates by retrograde transport of adeno-associated virus (AAV) particles injected intramuscularly.[23,24] Gene delivery of NpHR has shown high and well-tolerated neuron-specific expression in nonhuman primates,[25] and clinical trials of gene delivery using a variety of AAV serotypes in humans are underway.[26–29] Future advances in gene-delivery techniques could achieve selective delivery of NpHR to nontransgenic motor neurons in humans. Demonstration of long-term safety and efficacy in combination with advances in light delivery devices may enable clinical translation of robust, reversible, and selective optical inhibition in humans to treat spastic hypertonia.

Although there are many challenges associated with the translation of this technique to humans, the demonstration of optical inhibition of motor nerve and muscle activity in transgenic mice provides a first step toward novel optogenetics-based therapies for spastic hypertonia associated with upper motor neuron syndrome and hypertonicity associated with a wide range of other diseases.

The authors thank M. Llewellyn, K. Thompson, and D.C. Lin for technical assistance and K. McGill for valuable discussions.

REFERENCES

1. Katz RT, Rymer WZ. Spastic hypertonia: mechanisms and measurement. Arch Phys Med Rehabil 1989;70:144–155.
2. McClelland S, Teng O, Benson LS, Boulis NM. Motor neuron inhibition-based gene therapy for spasticity. Am J Phys Med Rehabil 2007;86:412–421.
3. Simon O, Yelnik AP. Managing spasticity with drugs. Eur J Rehabil Med 2010;46:401–410.
4. Sheean G, McGuire JR. Spastic hypertonia and movement disorders: pathophysiology, clinical presentation, and quantification. PM R 2009;1:827–833.
5. Fenno L, Yizhar O, Deisseroth K. The development and application of optogenetics. Ann Rev Neurosci 2011;34:389–412.
6. Boyden ES, Zhang F, Bamberg E, Nagel G, Deisseroth K. Millisecond-timescale, genetically targeted optical control of neural activity. Nat Neurosci 2005;8:1263–1268.
7. Zhang F, Wang LP, Brauner M, Lewald JF, Kay K, Watzke PG, et *al.* Multimodal fast optical interrogation of neural circuitry. Nature 2007;446:633–639.
8. Llewellyn ME, Thompson KR, Deisseroth K, Delp SL. Orderly recruitment of motor units under optical control in vivo. Nat Med 2010;16:1161–1165.
9. Bruegmann T, Malan D, Hesse M, Beiert T, Fuegemann CJ, Fleischmann BK, et *al.* Optogenetic control of heart muscle in vitro and in vivo. Nat Methods 2010;11:897–900.
10. Kanbar R, Stornetta RL, Cash DR, Lewis SJ, Guyenet PG. Photostimulation of Phox2b medullary neurons activates cardiorespiratory function in conscious rats. Am J Respir Crit Care Med 2010;82:1184–1194.
11. Sharp AA, Fromherz S. Optogenetic regulation of leg movement in midstage chick embryos through peripheral nerve stimulation. J Neurophysiol 2011;106:2776–2782.
12. Gradinaru V, Thompson KR, Deisseroth K. eNpHR: a *Natronomonas* halorhodopsin enganced for optogenetic applications. Brain Cell Biol 2008;36:129–139.
13. Zhao S, Cunha C, Zhang F, Liu Q, Gloss B, Deisseroth K, et *al.* Improved expression of halorhodopsin for light-induced silencing of neuronal activity. Brain Cell Biol 2008;36:141–154.
14. Schneider CA, Rasband WS, Eliceiri KW. NIH Image to ImageJ: 25 years of image analysis. Nat Methods 2012;9:671–675.
15. Zhang F, Gradinaru V, Adamantidis AR, Durand R, Airan RD. de Lecea L, *et al.* Optogenetic interrogation of neural circuits: technology for probing mammalian brain structures. Nat Protoc 2010;5:439–456.
16. Gupta R, Nassiri N, Hazel A, Bathen M, Mozaffar T. Chronic nerve compression alters Schwann cell myelin architecture in a murine model. Muscle Nerve 2012;45:231–241.
17. Binding J, Arous JB, Léger J-F, Gigan S, Boccara C, Bourdieu L. Brain refractive index measured in vivo with high-NA defocus-corrected full-field OCT and consequences for two-photon microscopy. Opt Express 2011;19:4833–4847.
18. Liebregts MT, McLachlan RS, Leung LS. Hyperthermia induces age-dependent changes in rat hippocampal excitability. Ann Neurol 2002;52:318–326.
19. Aravanis AM, Wang LP, Zhang F, Meltzer LA, Mogri MZ, Schneider MB, et *al.* An optical neural interface: in vivo control of rodent motor cortex with integrated fiberoptic and optogenetic technology. J Neural Eng 2007;4(suppl):S143–156.
20. Bhadra N, Kilgore KL. High-frequency electrical conduction block of mammalian peripheral motor nerve. Muscle Nerve 2005;32:782–790.
21. Ackermann DM, Foldes EL, Bhadra N, Kilgore KL. Nerve conduction block using combined thermoelectric cooling and high frequency electrical stimulation. J Neurosci Methods 2010;193:72–76.
22. Gradinaru V, Mogri M, Thompson KR, Henderson JM, Deisseroth K. Optical deconstruction of parkinsonian neural circuitry. Science 2009;324:354–359.
23. Towne C, Schneider BL, Kieran D, Redmond DE Jr, Aebischer P. Efficient transduction of non-human primate motor neurons after intramuscular delivery of recombinant AAV serotype 6. Gene Ther 2010;17:141–146.
24. Hollis ER II, Kadoya K, Hirsch M, Samulski RJ, Tuszynski MH. Efficient retrograde neuronal transduction utilizing self-complementary AAV1. Mol Ther 2007;16:296–301.
25. Diester I, Kaufman MT, Mogri M, Pashaie R, Goo W, Yizhar O, et *al.* An optogenetic toolbox designed for primates. Nat Neurosci 2011;14:387–397.
26. Nathwani AC, Tuddenham EG, Rangarajan S, Rosales C, McIntosh J, Linch DC, et *al.* Adenovirus-associated virus vector-mediated gene transfer in hemophilia B. N Engl J Med 2011;365:2357–2365.
27. LeWitt PA, Rezai AR, Leehey MA, Ojemann SG, Flaherty AW, Eskandar EN, et *al.* AAV2-GAD gene therapy for advanced Parkinson's disease: a double-blind, sham-surgery controlled, randomised trial. Lancet Neurol 2011;10:309–319.
28. Flotte TR, Trapnell BC, Humphries M, Carey B, Calcedo R, Rouhani F, et *al.* Phase 2 clinical trial of a recombinant adeno-associated viral vector expressing α1-antitrypsin: interim results. Hum Gene Ther 2011;22:1239–1247.
29. Bowles DE, McPhee SW, Li C, Gray SJ, Samulski JJ, Camp AS, et *al.* Phase 1 gene therapy for Duchenne muscular dystrophy using a translational optimized AAV vector. Mol Ther 2012;20:443–455.